Soft Matter

Cite this: *Soft Matter*, 2012, **8**, 10636

www.rsc.org/softmatter

PAPER

Microfluidic synthesis of monodisperse porous microspheres with size-tunable pores

Wynter J. Duncanson,[a] Maximilian Zieringer,[a] Olaf Wagner,[b] James N. Wilking,[a] Alireza Abbaspourrad,[a] Rainer Haag[b] and David A. Weitz*[a]

Received 25th March 2012, Accepted 30th April 2012
DOI: 10.1039/c2sm25694k

We use a perfluorinated-dendrimer–dye complex that stabilizes microbubbles as a novel pore-forming agent. We use microfluidics to produce monodisperse emulsions containing a polymer matrix material, a model active, and the perfluorinated complex; upon drying, the emulsions form porous microspheres. This porosity causes the encapsulated model active to be released faster than from non-porous microspheres. Moreover, because of the fluorous features of the pores, we can also attach an additional guest molecule to the pores which is released with a profile that is distinct from that of the encapsulated active. These porous microspheres can encapsulate and controllably release multiple actives; this makes them valuable for applications such as drug delivery and imaging.

Introduction

Degradable porous polymer microspheres are promising vehicles for the encapsulation and delivery of actives such as gases,[1] drugs,[2] enzymes, and catalysts.[3] The introduction of porosity in microspheres requires the use of pore-forming agents; during synthesis, they are emulsified with the other microsphere components. Commonly used pore-forming agents, or porogens, include hydrocarbon waxes, carbohydrates, gelatin, ice, and sugars;[4–7] however, each of these must be removed in a second processing step to produce the pores and this requires a harsh leaching process. The pore-forming strategy involving these porogens has inherent limitations: leaching with solvents facilitates diffusional mass exchange which removes the porogen but also can remove encapsulated actives.[8,9] Moreover, the high-shear inherent in emulsification leads to microspheres with broad distributions in size and morphology and this can be further exacerbated by the inclusion of these porogens. These limitations can be overcome through the use of new synthesis strategies: for example, the polydispersity in particle size can be significantly reduced by using the capabilities of controlled production with microfluidic techniques.[10–14] In addition, traditional porogens can be replaced with new porogens that are permanent geometric templates or scaffolds and thus do not require leaching to produce pores;[14–16] moreover, these also add functionality to the matrix due to their composition. For example, protein-coated microbubbles can be used to form protein-coated pores in polymer scaffolds.[6,17,18] However, these new types of porogens have not been combined with microfluidics to produce porous microspheres. This combination would enable production of monodisperse porous microspheres with controllable size and morphology; furthermore, the use of these new porogens would eliminate the need for the second leaching step while enhancing the loading capabilities of the microspheres.

In this paper we evaluate the formation of pores using a permanent geometric template in porous monodisperse microspheres that are fabricated with a microfluidic device. As the porogen, we use a fluorous dendrimer–dye complex, and show that it forms discrete microbubbles in the matrix-forming polymer of the microspheres. We prepare monodisperse emulsions containing the matrix-forming polymer, the dendrimer–dye complex and an active molecule using a microfluidic device that produces single emulsions in a continuous process. These porogens eliminate the requirements for disruptive material removal, thereby enabling us to efficiently encapsulate active ingredients in the matrix. In addition, the resultant pores have perfluoro-alkyl moieties to which we non-covalently attach an additional guest-molecule by fluorous–fluorous interactions. We also demonstrate tunability of pore size through variation of the dendrimer–dye complex used.

Experimental section

Materials

Commercially available chemicals were purchased from reliable sources and used as delivered. Poly(DL-lactic acid) (PLA, M_w = 15 000 g mol^{-1}, Polysciences, Inc.) and Poly(DL-lactide/glycolide [50 : 50]) (PLGA, M_w = 12 000–16 500 g mol^{-1}, Polysciences, Inc.) were used as matrix-forming polymer for microspheres. Poly(vinyl alcohol) (PVA, M_w = 13 000–23 000 g mol^{-1}, 98%

[a]*School of Engineering and Applied Sciences, Harvard University, 29 Oxford St., Cambridge, MA 02138, USA. E-mail: weitz@deas.harvard.edu*
[b]*Freie Universität Berlin, Institute for Chemistry and Biochemistry, Takustrasse 3, D-14195 Berlin, Germany*

hydrolyzed, Aldrich) was used as surfactant (10% w/v) for the aqueous phase. Nile Red was used as hydrophobic dye for the inner oil phase. Dichloromethane (DCM, 99.8%, Mallinckrodt) served as an organic solvent for PLA or PLGA and Nile Red. The square microcapillaries were purchased from Atlantic International Technologies. The round glass microcapillaries were purchased from World Precision Instruments, Inc. and tapered using a Micropipette Puller from Shutter Instruments Co. All aqueous solutions were filtered by Acrodisc 32 mm syringe filters with 5 μm Supor membrane before use.

Microsphere fabrication

The microfluidic devices that were used for the microsphere fabrication consisted of a glass slide, Polyethylene or Teflon tubing (Scientific Commodities), square glass capillaries, round glass capillaries and syringe needle tips. The round tapered capillary was coated with the hydrophilic compound 2-[methoxy(polyethyleneoxy)-propyl]trimethoxysilane. The outer aqueous phase and inner oil phase were infused at independently adjustable flow rates using syringe pumps connected to the device by tubing. An aqueous 10 wt% PVA solution was used as the outer aqueous phase and a 5 wt% PLA solution in DCM with Nile Red (0.1–2 mM) was used as the inner oil phase. The drops were collected in an aqueous 2 wt% PVA solution. The DCM was removed under reduced pressure and the dried spheres were washed with deionized water to remove residual PVA.

Characterization

Optical and confocal microscopy images were obtained with a Leica TCS SP5 confocal microscope. A sample chamber was filled with the sonicated mixture of the dendrimer–dye complex, PLA, and DCM. The chamber was covered by Parafilm® to prevent solvent evaporation. Samples of dried spheres were imaged directly on microscope slides. Samples were loaded on double-sided carbon tape on an aluminium stud for scanning electron microscopy. Images of the uncoated samples were acquired with a Zeiss FESEM Supra55VP or Ultra scanning electron microscope using secondary electron detection at 1 kV. UV-Vis spectra were recorded with PerkinElmer UV/Vis Spectrometer Lamda 40. Maximum absorption at 538 nm in DCM was converted into Nile Red concentrations using a linear calibration plot of concentrations between 0.5 and 50 μM. The spectra were recorded at room temperature and were evaluated.

Fluorescence spectroscopy

Fluorescence emission spectra were acquired with PerkinElmer Luminescence Spectrometer LS 50B. Both excitation and emission slits were set at 10 nm. Excitation of samples at 488 nm was used to detect Nile Red and F-FITC. All measurements were conducted at room temperature.

The average diameter and coefficient of variation (CV) of the microbubbles were calculated from confocal microscopy images. The polydispersity was determined by measuring the diameter of over 300 spheres randomly selected from each sample. The average porosity was determined by calculating the air to total volume ratio of 20 cross-sections of multiple spheres that were randomly selected in each sample.

Release studies

PLGA porous and nonporous microspheres containing Nile Red were suspended in 1.5 mL of 0.1 M HCl solution. The suspension was incubated on a shaker at 37 °C. At predetermined intervals, the tube was centrifuged and 1.4 mL of the supernatant was collected and replaced with an equal volume of fresh 0.1 M HCl solution. The Nile Red of the collected supernatant was extracted with DCM and the concentration of Nile Red in DCM was quantified using UV-Vis spectroscopy. The percentage of active release at each time point was calculated by normalizing the obtained data with the cumulative total amount of active inside the particles. For the release experiment of F-FITC and Nile Red under neutral conditions, loading of the perfluoro-bi-tagged FITC was accomplished by incubation with a 1 mM F-FITC solution in perfluorohexane followed by washing with pure perfluorohexane. 7.1 mg of resulting microspheres were suspended in 1 mL pure water in a centrifuge tube. The centrifuge tube was incubated at 37 °C in a shaker. To collect the supernatant the tube was centrifuged and 0.9 mL of the supernatant were collected and replaced with an equal volume of distilled water. The dyes of the collected supernatant were extracted with DMSO. The concentration of Nile Red and F-FITC in DMSO was quantified using fluorescence spectroscopy.

Results and discussion

Fluorous compounds are organic molecules that carry one or more perfluoro-alkyl chains; these hydro- and lipophobic chains can aggregate or self-assemble in common solvents.[19–22] For example, dendrimers with perfluorinated shells form supramolecular complexes with perfluoro-tagged guest molecules in organic solvents; these complexes assemble around residual air to form stabilized microbubbles.[23] The dendrimer component consists of a perfectly branched polyglycerol (PG) core which is fully functionalized at the periphery with perfluoro-alkyl chains that form the shell, as sketched in Fig. 1a. Disperse Red 1 dye with a perfluoro-alkyl chain coupled to its hydroxy group, serves as the guest molecule, as sketched in Fig. 1b. We use two generations of PG dendrimers: generation 1.5 ([G1.5]) bears eight perfluoro-alkyl chains at the periphery, while generation 3.5 ([G3.5]) bears 32 chains. When either of these PGs with perfluorinated shells is combined with perfluoro-tagged Disperse Red in an organic solvent, fluorous attractions cause them to self-assemble and form stable gas-filled microbubbles as sketched in Fig. 1c.

These stabilized microbubbles can be incorporated into the microsphere formulation only if the dendrimer–dye complex self-assembles in presence of the matrix-forming polymer. To realize this concept, we combine the dendrimer–dye complex, dichloromethane, and a matrix-forming biodegradable polymer, poly(lactic acid) (PLA); Nile Red fluorescent dye is also added to the mixture to aid in visualization and to be a model active molecule. This solution is sonicated to induce the formation of stabilized microbubbles. The microbubbles are imaged with a confocal microscope; the background solution containing the matrix polymer and an organic solvent is red, whereas the stabilized bubbles appear as black areas as shown respectively for [G1.5] and [G3.5] dendrimer–dye complexes in Fig. 1d and e.

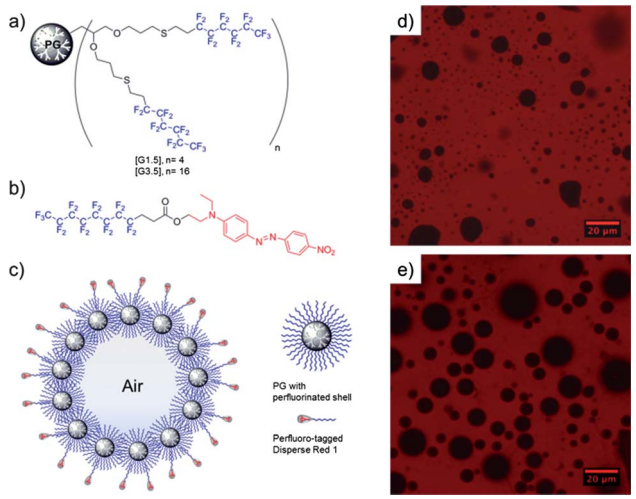

Fig. 1 (a) Sketch of perfectly branched perfluorinated PG dendrimer where $n = 4$ for [G1.5], and $n = 16$ for [G3.5]. (b) Sketch of perfluoro-tagged Disperse Red dye. (c) Schematic of stabilized microbubble formed through the self-assembly of the dendrimer–dye complex. (d) Fluorescence image of microbubbles stabilized by [G1.5]–dye complex in the presence of matrix-forming polymer, PLA. (e) Fluorescence image of microbubbles stabilized by [G3.5]–dye complex in the presence of matrix-forming polymer, PLA.

Thus, the addition of the PLA to the dendrimer–dye complex does not interfere with the microbubble self-assembly process. To quantify microbubble size, we analyze the images with ImageJ and calculate the microbubble diameters; we find values of 2.47 ± 1.57 μm for the smaller dendrimer, generation [G1.5], and 6.58 ± 2.49 μm for the larger dendrimer, generation [G3.5]. The increase in the microbubble diameter between generation numbers can be attributed to the differences in solubility: higher solubilities of [G1.5] in DCM lead to the formation of smaller aggregates, while lower solubilities of [G3.5] lead to the formation of larger aggregates.[23] The microbubble stabilization provided by the dendrimer–dye complexes in the presence of matrix-forming polymer enables the use of this architecture as a porogen; moreover, the variation in microbubble size using the different dendrimer generations can be exploited to adjust porosity.

Polymer microspheres containing the dendrimer–dye complex are generated in glass-capillary microfluidic devices that have a flow-focusing geometry in which a round tapered capillary is coaxially aligned within a square capillary. The dispersed phase enters the device from one end of the square capillary and is flow-focused into the tapered orifice of the round capillary by the continuous phase, which is input from the other end. Monodisperse drops are produced at the orifice of the round tapered capillary, as shown in the schematic in Fig. 2a. The microfluidic devices provide perfect control over the fabrication of the drops, producing a continuous stream of PLA drops which are monodisperse, as shown in Fig. 2b. We produce drops containing either [G1.5], or [G3.5]; as a control we also make drops with no dendrimer–dye complex. We collect the drops and remove the organic solvent, residual water, and gas through application of a vacuum; this dries the drops causing them to become solid microspheres.

To evaluate the effect of the dendrimer–dye complex on the size and morphology distributions of the microspheres, we analyze optical microscopy images of dried microspheres; we find that the coefficient of variation (CV) values for the microsphere diameters is less than 6% for the three types of microspheres, indicating the high uniformity of their sizes. In addition, we compare the size distributions of the three types of microspheres by a student's *t*-test, and find the size distributions are not significantly different, thereby validating that addition of dendrimer does not affect the microsphere size distribution. By contrast, addition of the dendrimer does affect the porosity of the microspheres as is evident by comparison of the SEM images; the dried microspheres formed with the dendrimer–dye complexes are porous as shown in Fig. 2b and c whereas those made without the complex are non-porous as shown in Fig. 2d. Therefore, the self-assembling dendrimer–dye complex is a porogen that yields pores upon microsphere drying; leaching is not required for pore-formation. Since, the dendrimer–dye complex is a scaffold for pores, we also expect the size of the pores in the dried microspheres will be proportional to the size of the bubbles formed by the dendrimer–dye complex in solution. To confirm this, we compare the pore sizes in the dried microspheres produced from the two generations of PG dendrimers and find that the pores formed by the [G1.5] are smaller than those formed by the [G3.5] as shown in Fig. 2b and c. Thus, the dendrimer–dye complex can be used as a permanent porogen to form pores in microspheres and the pore-size can be changed by increasing the dendrimer generation from 1.5 to 3.5.

The use of the perfluorinated dendrimer–dye complex provides an additional benefit due to its fluorous groups. In solution, the dendrimer–dye complex–gas interface is lined with perfluoroalkyl chains; as a result, perfluorinated-alkyl-chains of the complex are oriented toward the gas phase of the microbubbles. Because the microbubbles maintain their integrity, the pores should also remain perfluorinated. This allows us to immobilize perfluoro-tagged guest molecules in the pores through fluorous–fluorous interactions. To demonstrate this additional functionality, we attach a bi-perfluoro-tagged fluorescein isothiocyanate (F-FITC) to the pores by adding it to the [G3.5] microsphere suspension, as sketched in Scheme 1.

The [G3.5] microspheres are incubated and then washed with perfluorohexane to remove any unbound F-FITC. The microsphere morphology and the locations of the dye-labeled molecules are visualized with confocal microscopy. The microspheres are porous as evidenced by the black voids in the red microsphere matrix shown in Fig. 3a. We image the F-FITC separately and find that the pore space appears to be coated by the F-FITC as shown in Fig. 3b. The location of the pores is clarified in an overlay of the red and green images of the microsphere surface which shows the green dye overlaps the black voids in the red microsphere as shown in Fig. 3c. The immobilization of F-FITC in the pores can only be explained by the fluorous–fluorous non-covalent binding between it and the fluorinated pores. Moreover, from the analysis of the spatial profiles of the fluorescence in Fig. 3d, we find that the microsphere body itself exhibits only red fluorescence, whereas the surface region exhibits both red and green fluorescence, as shown in Fig. 3e. This confirms that the resultant porous microspheres are loaded with two active ingredients; one is encapsulated in the microsphere matrix and the other is on the surface pores.

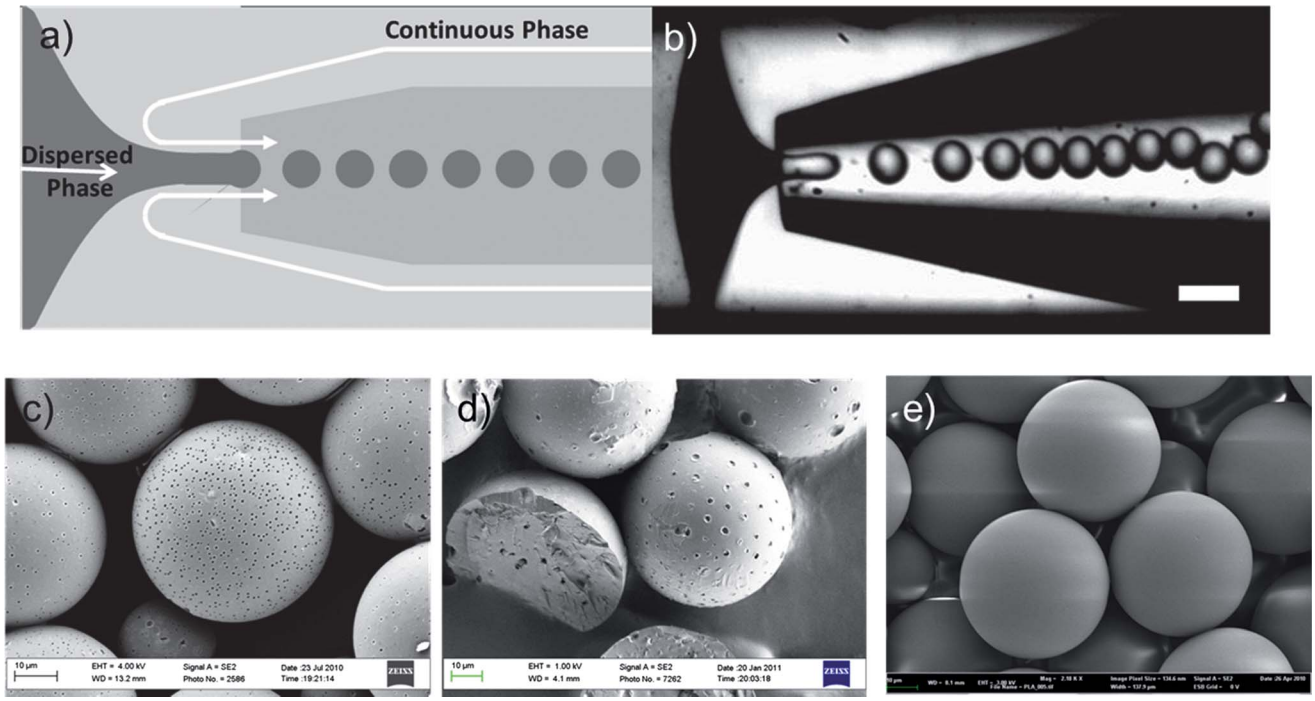

Fig. 2 (a) Schematic of flow-focusing glass-capillary device. (b) Optical image of drop formation in glass microcapillary device. Scale bar is 200 μm. Scanning electron micrographs of PLA microspheres made (c) with [G1.5]–dye complex, (d) [G3.5]–dye complex and (e) without dendrimer–dye complex.

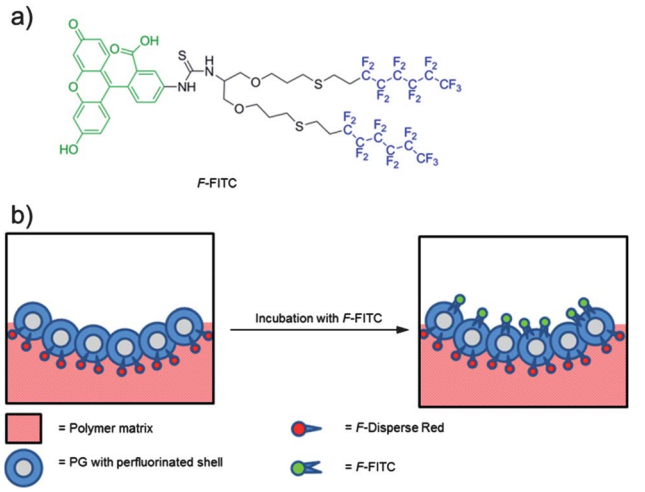

Scheme 1 (a) Molecular structure of F-FITC. (b) Illustration of pore surface functionalization by incubation with F-FITC.

Release of actives occurs through polymer degradation which occurs by ester hydrolysis.[24] Degradation is more rapid for large surface areas; therefore, porous microspheres are expected to have a faster degradation rate.[7,25,26] This degradation can be further accelerated in acidic solutions and through replacement of PLA by the faster degrading copolymer, poly(lactic-*co*-glycolic acid) (PLGA).[24] We measure the cumulative release of the actives over the course of 40 days as the PLGA microspheres degrade in an acidic aqueous phase, made with 0.1 M HCl. We find that the porous microspheres made with [G3.5] release the Nile Red active more rapidly than do the microspheres of the same diameter but with no pores, as shown in Fig. 4.

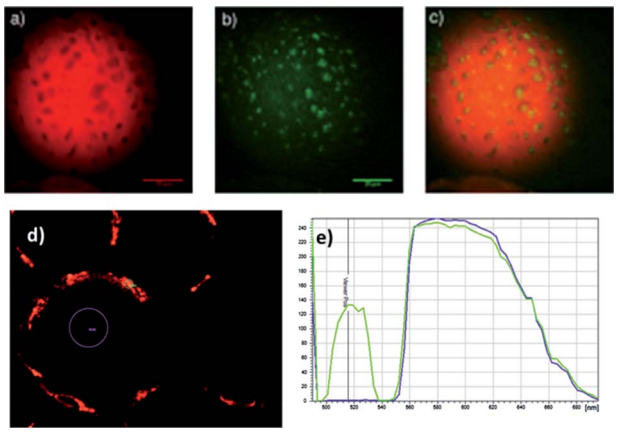

Fig. 3 (a) Confocal micrograph of the Nile Red labelled porous PLA microsphere formed with [G3.5]–dye complex. (b) Confocal micrograph of the F-FITC on the pores of the porous microsphere. (c) Overlay of red and green images. (d) Confocal microscopy cross-section of F-FITC loaded porous microsphere. (e) Corresponding fluorescence intensity over wavelength graphs of microsphere body (blue) and surface (green).

Initially, in the first four days, the release is faster because of the contribution of the surface associated actives; however, the release rate slows as the actives in the bulk matrix are released. Though the initial release of the Nile Red is only ~4% for the porous microspheres, it is still greater than the ~3% release from the non-porous microspheres. Furthermore, after 40 days, 17.2 ± 4.1% of the Nile Red has been released from the porous microspheres, by contrast only 10.8 ± 2.8% of the Nile Red has been released from the non-porous microspheres; this pronounced

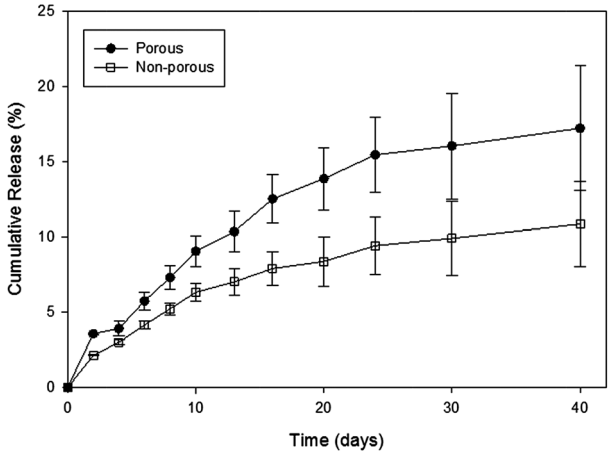

Fig. 4 Cumulative release of Nile Red from porous (black circles) and non-porous (open squares) PLGA microspheres in 0.1 M HCl.

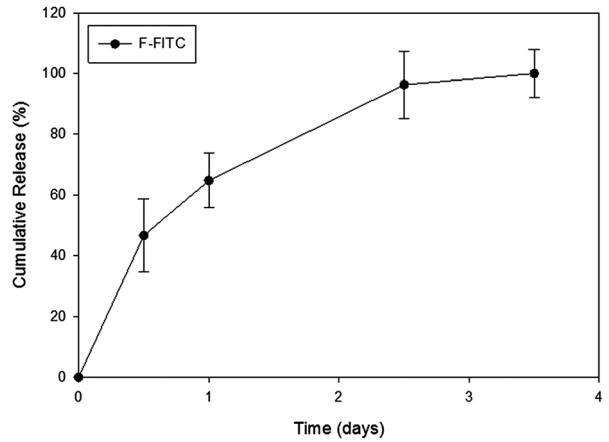

Fig. 5 Cumulative release of F-FITC from porous PLGA microspheres in 0.1 M HCl.

increase reflects the effects of the pores formed by the dendrimer–dye complex. Moreover, we also observe complete release of the F-FITC within four days, as demonstrated in Fig. 5. Interestingly, the F-FITC release-time corresponds to the surface-associated surface release time of four days; this further validates that the F-FITC was located only on the microsphere surface.

Conclusions

In summary, we have used a self-assembling dendrimer–dye complex as a permanent porogen to produce monodisperse biodegradable porous microspheres with well-defined pores. This porogen not only forms pores, it is also a carrier for additional active materials. The porosity accelerates the degradation of the microsphere structure to accelerate the release of molecules from the microsphere matrix. Furthermore, the pores retain their fluorinated activity making it possible to also carry perfluorinated compounds on the microsphere surface. Our pore-forming approach using the dendrimer–dye complex also provides a new strategy to release two types of actives from the same microsphere, each with a distinct time-scale. These new multi-active microspheres can carry both perfluorinated gas and a hydrophobic drug. This could enable a unique new application; they could be used for simultaneous ultrasound monitoring and drug delivery.

Acknowledgements

This work was supported by the Advanced Energy Consortium. Member companies include BP America Inc., Baker Hughes Inc., Conoco-Phillips, Halliburton Energy Services Inc., Marathon Oil Corp., Occidental Oil and Gas, Petrobras, Schlumberger, Shell, and Total. M.Z., O.W., and R.H. are indebted to the Center for International Cooperation (FU Berlin) and the graduate school "Fluorine as a Key Element" (GRK 1582) funded by the German Science Foundation (DFG).

Notes and references

1 J. A. Straub, D. E. Chickering, C. C. Church, B. Shah, T. Hanlon and H. Bernstein, *J. Controlled Release*, 2005, **108**, 21–32.
2 J. A. Straub, D. E. Chickering, T. G. Hartman, C. A. Gloff and H. Bernstein, *Int. J. Pharm.*, 2007, **328**, 35–41.
3 M. T. Gokmen, W. Van Camp, P. J. Colver, S. A. F. Bon and F. E. Du Prez, *Macromolecules*, 2009, **42**, 9289–9294.
4 T. K. Kim, J. J. Yoon, D. S. Lee and T. G. Park, *Biomaterials*, 2006, **27**, 152–159.
5 Z. Ma, C. Gao, Y. Gong and J. Shen, *J. Biomed. Mater. Res., Part B*, 2003, **67**, 610–617.
6 J. Li, Y. Chen, A. F. Mak, R. S. Tuan, L. Li and Y. Li, *Acta Biomater.*, 2010, **6**, 2013–2019.
7 M. M. Arnold, E. M. Gorman, L. J. Schieber, E. J. Munson and C. Berkland, *J. Controlled Release*, 2007, **121**, 100–109.
8 Y. Yang, N. Bajaj, P. Xu, K. Ohn, M. D. Tsifansky and Y. Yeo, *Biomaterials*, 2009, **30**, 1947–1953.
9 H. R. Lin, C. J. Kuo, C. Y. Yang, S. Y. Shaw and Y. J. Wu, *J. Biomed. Mater. Res.*, 2002, **63**, 271–279.
10 L.-Y. Chu, J.-W. Kim, R. K. Shah and D. A. Weitz, *Adv. Funct. Mater.*, 2007, **17**, 3499–3504.
11 X. Gong, W. Wen and P. Sheng, *Langmuir*, 2009, **25**, 7072–7077.
12 Z. Nie, S. Xu, M. Seo, P. C. Lewis and E. Kumacheva, *J. Am. Chem. Soc.*, 2005, **127**, 8058–8063.
13 S. Dubinsky, J. I. Park, I. Gourevich, C. Chan, M. Deetz and E. Kumacheva, *Macromolecules*, 2009, **42**, 1990–1994.
14 S.-W. Choi, Y. Zhang and Y. Xia, *Adv. Funct. Mater.*, 2009, **19**, 2943–2949.
15 S. E. Bae, J. S. Son, K. Park and D. K. Han, *J. Controlled Release*, 2009, **133**, 37–43.
16 K. Naidoo, H. Rolfes, K. Easton, S. Moolman, A. Chetty, W. Richter and R. Nilen, *Mater. Lett.*, 2008, **62**, 252–254.
17 A. Nair, P. Thevenot, J. Dey, J. Shen, M.-W. Sun, J. Yang and L. Tang, *Tissue Eng., Part C*, 2010, **16**, 23–32.
18 D. L. Elbert, *Acta Biomater.*, 2011, **7**, 31–56.
19 V. Percec, D. Schlueter, Y. K. Kwon and J. Blackwell, *Macromolecules*, 1996, **28**, 8807–8818.
20 V. Percec, G. Johansson, G. Ungar and J. Zhou, *J. Am. Chem. Soc.*, 1996, **118**, 9855–9866.
21 G. Johansson, V. Percec, G. Ungar and J. Zhou, *Macromolecules*, 1996, **29**, 646–660.
22 C. J. Wilson, D. A. Wilson, A. E. Feiring and V. Percec, *J. Polym. Sci., Part A: Polym. Chem.*, 2010, **48**, 2498–2508.
23 M. Zieringer, A. Garcia-Bernabé, B. Costisella, H. Glatz, W. Bannwarth and R. Haag, *ChemPhysChem*, 2010, **11**, 2617–2622.
24 J. M. Anderson and M. S. Shive, *Adv. Drug Delivery Rev.*, 1997, **28**, 5–24.
25 M. L. Houchin and E. M. Topp, *J. Pharm. Sci.*, 2008, **97**, 2395–2404.
26 R. C. Mundargi, V. R. Babu, V. Rangaswamy, P. Patel and T. M. Aminabhavi, *J. Controlled Release*, 2008, **125**, 193–209.

